Investigating the period of oscillation and the angle of an inclined spring mass system

How does the angle between the vertical plane and the inclined pendulum connected to a spring affect its period of oscillation?

International Baccalaureate Extended Essay

Physics

Word Count: 3979

Contents

1 Introduction

Gravity is always considered the constant in experiments that allow the relationship between two variables to be determined. It is used when the simple pendulum is studied in introductory physics laboratories. Despite being studied extensively throughout the decades and being one of the earliest instruments to measure the effects of gravity; however, it had only been under the effects of Earth's gravitational field. As a result, we wondered whether there was a way of investigating the pendulum's behavior under a different gravitational field strength. One way is by a "variable gravity pendulum" (Feliciano 3), which alters the geometry of a traditional physical pendulum system and allows it to swing in a non-vertical plane, simulating the effects of different gravitational field strengths.

Since the simple pendulum is not a rigid body, it is not able to swing in a non-vertical plane, therefore, we looked into using a physical pendulum instead. The physical pendulum is a better choice because it is a rigid body that undergoes a fixed-axis rotation about a pivot point (Lehman 3), only allowing one degree of freedom no matter its geometry. In addition, a spring connected to a pendulum changes its motion, so we decided to add a spring to our system. All of these lead to the question: How does the angle between the vertical plane and the inclined pendulum connected to a spring affect its period of oscillation? This paper aims to develop a mathematical model that describes the motion of our pendulum system and verify its accuracy with experimental results.

2 Background Information

In the ideal situation where the pendulum is in a vacuum, its motion will continue indefinitely, which we refer to as Simple Harmonic Motion (SHM). It has the defining property that its acceleration is negatively proportional to the displacement from the equilibrium, $a \propto -x$. However, it is not valid to apply an idealized model to reality. As mentioned previously, we are studying the oscillation of a physical pendulum in a medium; this implies that factors like air resistance or other frictions will eventually bring its oscillatory motion to an end. This phenomenon is known as Damped Harmonic Motion (DHM), and we encounter this phenomenon because our pendulum system operates in the air under the presence of air drag. Air drag is a resistance and non-conservative force that dissipates the energy from the system, primarily thermal energy, to the surroundings (Tsokos 49-50). This phenomenon can be described mathematically using Newton's second law, with an additional term that accounts for decaying the oscillating motion. For an object traversing in a medium at a moderate velocity, the drag force is approximated to be proportional to the velocity, $F_D \propto v$, where through

the drag coefficient b, the drag force can be written as $F_D = -bv$ (LibreTexts). The drag coefficient is a constant that depends on the dimensions of the body and properties of the medium (i.e., density, viscosity, or compressibility); the negative sign tells us that the drag force has a direction that is always opposite to that of the motion. This concept can be illustrated with the most common example: a horizontal spring-mass system experiencing a drag force, as shown in Figure. 1,

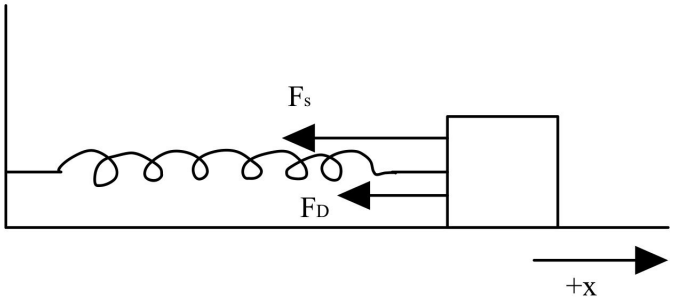

Figure 1: A horizontal spring mass system experiences a drag force F_D, resulting in damped harmonic oscillation. The direction of motion is also shown with $+x$.

We can construct the equation of motion using Newton's Second Law and Hooke's Law:

$$m\frac{d^2x}{dt^2} = -kx - bv$$

Dividing both sides by m and rearranging all the terms on the left hand side (LHS):

$$\frac{d^2x}{dt^2} + \frac{b}{m}\frac{dx}{dt} + \frac{k}{m}x = 0$$

To simplify the above expression, we let $2\beta = \frac{b}{m}$ and $\omega_0^2 = \frac{k}{m}$:

$$\frac{d^2x}{dt^2} + 2\beta\frac{dx}{dt} + \omega_0^2 x = 0 \tag{1}$$

The ansatz (educated guess) for this second order homogeneous linear differential equation takes the form of an exponential function, $x = Ae^{\alpha t}$. Substituting this gives us:

$$\frac{d^2}{dt^2}\left(Ae^{\alpha t}\right) + 2\beta\frac{d}{dt}\left(Ae^{\alpha t}\right) + \omega_0^2\left(Ae^{\alpha t}\right) = 0$$

Differentiating and simplifying these parameters result in a quadratic equation, as $Ae^{\alpha t}$ cannot be zero:

$$Ae^{\alpha t}(\alpha^2 + 2\beta\alpha + \omega_0^2) = 0$$

Where the two roots are $\alpha_1 = -\beta + \sqrt{\beta^2 - \omega_0^2}$ and $\alpha_2 = -\beta - \sqrt{\beta^2 - \omega_0^2}$, substituting back gives us:

$$x(t) = e^{-\beta t}(A_1 e^{\sqrt{\beta^2 - \omega_0^2}} + A_2 e^{-\sqrt{\beta^2 - \omega_0^2}})$$

For further simplification, we assign $\omega_1^2 = \omega_0^2 - \beta^2$, which in terms of complex exponential, becomes:

$$x(t) = e^{-\beta t}(A_1 e^{i\omega_1 t} + A_2 e^{-i\omega_1 t})$$

Since the solution is still complex, the condition to make the imaginary part disappear is that we assume the constants A_1 and A_2 to be complex conjugates that take the form, $\frac{1}{2}Ae^{i\phi}$ and $\frac{1}{2}Ae^{-i\phi}$ respectively:

$$x(t) = \frac{1}{2}Ae^{-\beta t}(e^{i(\omega_1 t + \phi)} + e^{-i(\omega_1 t + \phi)})$$

Using the identity that $\dfrac{e^{ix} + e^{-ix}}{2} = \cos x$ we reduce our model to:

$$x(t) = Ae^{-\beta t}\cos(\omega_1 t + \phi) \tag{2}$$

Finally, upon substituting $\beta = \dfrac{b}{2m}$ and $\omega_1 = \sqrt{\omega_0^2 - \beta^2}$, we get the general solution for damped harmonic motion:

$$x(t) = Ae^{-\frac{b}{2m}t}\cos\left(\sqrt{\frac{k}{m} - \frac{b^2}{4m^2}}t + \phi\right) \tag{3}$$

Where A is the maximum amplitude of the oscillation, ϕ is the phase shift that depends on the initial condition. This solution will be further applied in Section. 3 for the mathematical model of our investigation.

3 The Experiment

This section explores our system's specific experimental setup and mathematical model. Two modifications were made to the traditional pendulum system: first, inclining the physical pendulum to be at an angle with the vertical plane; second, having a spring that connects the pendulum to a wall. A front view of the setup can be seen in Figure 2,

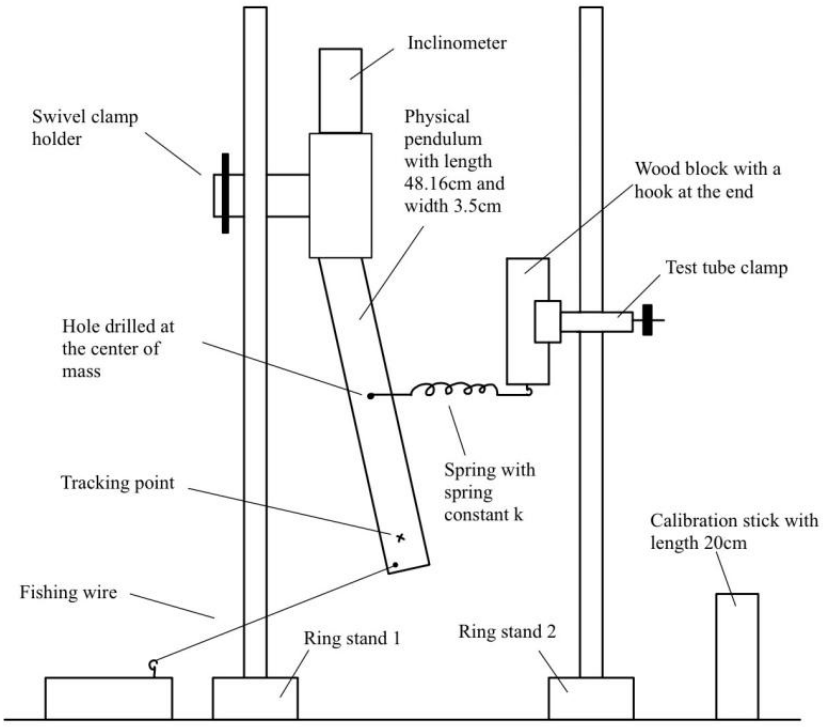

Figure 2: A front view of the pendulum system featuring the spring and initial release mechanisms.

A rectangular physical pendulum is clamped to a ring stand (labelled ring stand 1) through a swivel clamp holder (see Figure 3 for more details), and two holes are drilled using a drill press. One is drilled at the center of mass, 24.08cm from the bottom of the pendulum in length and 1.75cm from the edge in width. The location of this hole is based on the assumption that the center of mass is at the center of the rectangular pendulum. The other hole is drilled arbitrarily at the bottom left, as it does not have to be at a specific location due to its purpose of releasing the pendulum. A point is marked in red with a marker to provide a consistent tracking point when processing the motion on Tracker (see Section 5). An inclinometer is calibrated on a table to ensure it is returning a reading of 0° on the horizontal surface and is then taped at the top of the pendulum. This allows for more precise adjustments of different inclination angles.

Another ring stand (labelled ring stand 2) is placed to the right of the pendulum, where a wood block with a hook at the end is clamped using a test tube clamp. This acts as "a wall" that the spring will connect to with the pendulum's drilled hole at the center. It is also ensured that the spring is parallel to that of the table by adjusting the height of the wood block. To release the pendulum and provide it with an initial amplitude of roughly 14°, a wood block is placed 12cm to the left of the the ring stand 1. A fishing wire connects the wood block with the bottom drilled hole of the pendulum, which will be cut before the start of each trial. Lastly, another wood block with length 20cm is used

as a calibration stick to calibrate the video scale when processing. Some other experimental setup is only visible when we look at it in the side view as shown in Figure 3,

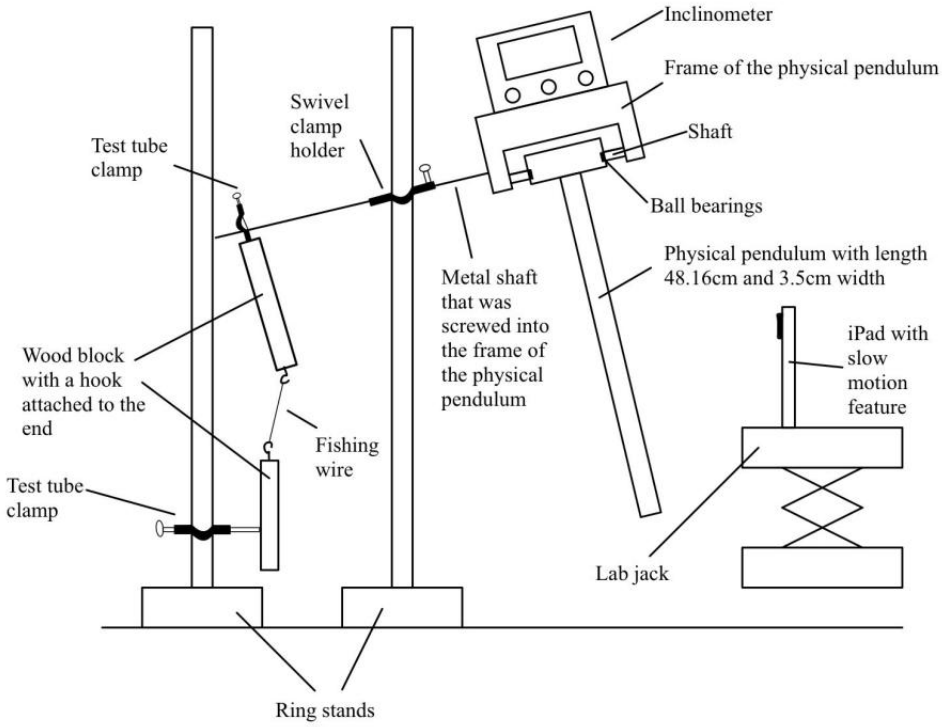

Figure 3: A side view of the pendulum featuring a counterweight and the pendulum installation mechanism.

The pendulum is installed by screwing a shaft through the physical pendulum and its frame, with ball bearings along the shaft to reduce friction at the pivot point. A metal shaft is screwed into the frame, which allows for the pendulum to be clamped to a ring stand using a swivel clamp holder. This clamp allows for its angle to be adjusted from the vertical up to 360° while being held in place. Since it is noticed that at higher angles, the clamp can not withstand the weight of the pendulum, a counterweight is employed. Two wood blocks that connects with the metal shaft allows the system to be stabilized at the specific angle throughout its motion. Lastly, an iPad, recording at 120 frames per second, is placed on a lab-jack for more convenient adjustment of heights.

We changed the angle of inclination of the pendulum by adjusting the swivel clamp holder according to the reading shown in the inclinometer. We experimented with 8 different angles: $0° - 70°$ in increments of 10°. At different inclination angles, we had to adjust ring stand 2 accordingly to ensure that the spring was connected parallel to the table. The counterweight was also adjusted before the start of each trial to eliminate fluctuations in the inclination angle. With the fishing wire, the pendulum was tied to the wood block to control the initial amplitude. The pendulum was released

by cutting the fishing wire using a pair of scissors while simultaneously starting to record on the iPad until the motion came to an end. This experiment was conducted three times for each inclination angle to reduce random errors.

We can now move on to derive the mathematics behind our experiment. However, since we have a rotating rigid body, we must first understand the concept of torque. Torque is the rotational equivalence of force and is quantified very similarly. It changes the rotational motion of objects that are rotating about an axis (Ling 508-509). It is a vector quantity denoted as $\vec{\tau}$ and is defined as,

$$\vec{\tau} = \vec{r} \times \vec{F} \tag{4}$$

Where it is a cross product between $\vec{r}$, the position vector from the pivot point to the point of contact of the applied force, and $\vec{F}$, the applied force vector. There is also a Newton's Second Law for rotational motion, which is,

$$\vec{\tau}_{net} = I\vec{\alpha} \tag{5}$$

Where the net torque equals to the product between the moment of inertia I (see Section. 10) and $\vec{\alpha}$, the angular acceleration. Before moving on, we must identify the different forces acting on the pendulum as seen in Figure. 4,

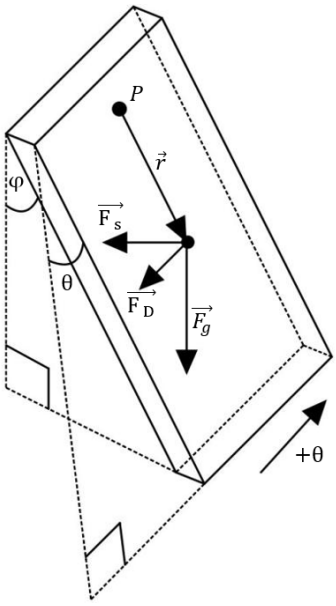

Figure 4: Isometric view of the pendulum showing the three forces and the angle φ made between the vertical plane, and the angular displacement denoted θ.

The three forces acting on the system are: the gravitational force F_g, which always point in the

direction perpendicular to the table; the spring force F_s, which points in the direction parallel to the table; the drag force F_D, which points in the opposite direction of angular displacement. The angle that we are varying in this system is denoted φ and the angular displacement denoted θ. Since the gravitational force is not acting in the same plane as the other forces, we can make a correction by letting $F_g' = F_g \cos\varphi$. This makes the gravitational force co-planar with the other forces. We can then reduce Figure 4 to a two-dimensional figure as shown in Figure 5,

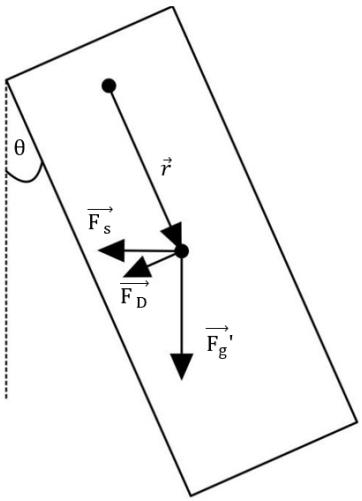

Figure 5: 2D view of the pendulum that shows the position vector and force vectors

Figure 5 shows the direction of the forces and the direction of the position vector. We can now compute the three torques using the right hand rule. Using the definition of torque, the torque generated by the spring force is:

$$\vec{\tau}_s = \vec{r} \times \vec{F}_s$$

Where using the right hand rule gives us:

$$\vec{\tau}_s = |\vec{r}||\vec{F}_s| \sin\left(\frac{\pi}{2} + \theta\right) \otimes$$

The torque by gravitational force is written as:

$$\vec{\tau}_g' = |\vec{r}||\vec{F}_g'| \sin(\theta) \otimes$$

The torque by drag force is written as:

$$\vec{\tau}_D = |\vec{r}||\vec{F}_D| \sin\left(\frac{\pi}{2}\right) \otimes$$

Since all the torques are of the same direction, the magnitude of the net torque can be written as the sum of all the magnitude of the torques:

$$|\vec{\tau}_{net}| = |\vec{r}||\vec{F}_s| \sin\left(\frac{\pi}{2} + \theta\right) + |\vec{r}||\vec{F}'_g| \sin(\theta) + |\vec{r}||\vec{F}_D| \sin\left(\frac{\pi}{2}\right)$$

We introduce a negative sign as we assume that a negative torque provides the conventional $+\theta$ to the right. From Eq.5, the net torque can be written in terms of angular acceleration. The forces can also be rewritten, where $|\vec{F}_s| = k(x - x_0)$; $|\vec{F}'_g| = mg\cos\varphi$; and $|\vec{F}_D| = bv$, where v in this case is written as the angular velocity $\dfrac{d\theta}{dt}$:

$$-I\frac{d^2\theta}{dt^2} = rk(x - x_0)\cos\theta + rmg\cos\varphi\sin\theta + rb\frac{d\theta}{dt}$$

Since the spring is noticed to have already been stretched at its equilibrium position, $x_0 \neq 0$. It can be adjusted by writing it in terms of θ:

$$I\frac{d^2\theta}{dt^2} = -kr(r\sin\theta - r\sin\theta_0) - mgr\cos\varphi\sin\theta - br\frac{d\theta}{dt}$$

Where θ_0 is the angle relative to the unstretched position of the spring. Since our maximum amplitude is defined to be relatively small in Section 3, we can apply small angle approximations to the angular displacement, θ, where $\cos\theta \approx 1$ and $\sin\theta \approx \theta$:

$$0 = I\frac{d^2\theta}{dt^2} + br\frac{d\theta}{dt} + kr^2\theta + mgr\cos\varphi\theta - kr^2\sin\theta_0$$

$$0 = \frac{d^2\theta}{dt^2} + \frac{br}{I}\frac{d\theta}{dt} + \frac{kr^2 + mgr\cos\varphi}{I}\theta - \frac{kr^2\sin\theta_0}{I}$$

This non-homogeneous second order differential equation can be solved by changing its coordinate system; however, we can assign a variable to each coefficient for simplicity:

$$0 = \frac{d^2\theta}{dt^2} + \underbrace{\frac{br}{I}}_{=2\beta}\frac{d\theta}{dt} + \underbrace{\frac{kr^2 + mgr\cos\varphi}{I}}_{=\omega_0^2}\theta - \underbrace{\frac{kr^2\sin\theta_0}{I}}_{=c}$$

The differential equation now looks like:

$$0 = \frac{d^2\theta}{dt^2} + 2\beta\frac{d\theta}{dt} + \omega_0^2\theta - c$$

We can factor an ω_0^2 from the last two terms:

$$0 = \frac{d^2\theta}{dt^2} + 2\beta\frac{d\theta}{dt} + \omega_0^2\left(\theta - \frac{c}{\omega_0^2}\right)$$

We assign a new coordinate system, P, where $P = \theta - \frac{c}{\omega_0^2}$:

$$0 = \frac{d^2P}{dt^2} + 2\beta\frac{dP}{dt} + \omega^2 P$$

This expression resembles the form of Eq. 1, which takes the general solution:

$$P(t) = P_{max}e^{-\beta t}\cos(\omega_1 t + \alpha)$$

Here, we can simply substitute $P = \theta - \frac{c}{\omega_0^2}$ back into the above expression to and solve for θ, giving us:

$$\theta(t) = \theta_{max}e^{-\beta t}\cos(\omega_1 t + \alpha) + \frac{c}{\omega_0^2}$$

Finally, we substitute all the variables and solve for $\frac{c}{\omega_0^2}$ to obtain the final equation of motion for our pendulum system:

$$\theta(t) = \theta_{max}e^{-\frac{br}{2I}t}\cos\left(\sqrt{\frac{kr^2 + mgr\cos\varphi}{I} - \left(\frac{br}{2I}\right)^2}\,t\right) + \frac{kr^2\sin\theta_0}{kr^2 + mgr\cos\varphi} \tag{6}$$

In Eq. 6, we neglected the phase shift α due to our initial condition that at time $t = 0$, our angular displacement is at $\theta = 0$. We can determine the damped frequency of our system that includes the damping coefficient $\left(\frac{br}{2I}\right)^2$ inside the cosine function, deviating from the system's natural frequency under the absence of air.

$$\omega_1 = \sqrt{\frac{kr^2 + mgr\cos\varphi}{I} - \left(\frac{br}{2I}\right)^2} \tag{7}$$

Here, we can determine the period of oscillation using $T = \frac{2\pi}{\omega_1}$,

$$T = \frac{2\pi}{\sqrt{\frac{kr^2 + mgr\cos\varphi}{I} - \left(\frac{br}{2I}\right)^2}} \tag{8}$$

The above equation suggests the relationship between the period of oscillation and the inclination angle. We can verify this equation by reverting the changes we made to our pendulum. If we let $\varphi = 0$, then $\cos\varphi = 1$, which removes the inclination of our pendulum. As for the spring, we let

$k = 0$, then the term $kr^2 = 0$. This leaves us with the period of a physical pendulum if air resistance is negligible ($b = 0$):

$$T = \frac{2\pi}{\sqrt{\frac{mgr}{I}}}$$

From Eq 8, we can expect that for greater φ, $\cos\varphi$ decreases; since the denominator decreases, the period T increases.

4 Calibration

In the previous section, we encounter two quantities: spring constant and moment of inertia, which are determined through an experiment and theory respectively. We determine the spring constant with a simple setup as shown in Figure. 6,

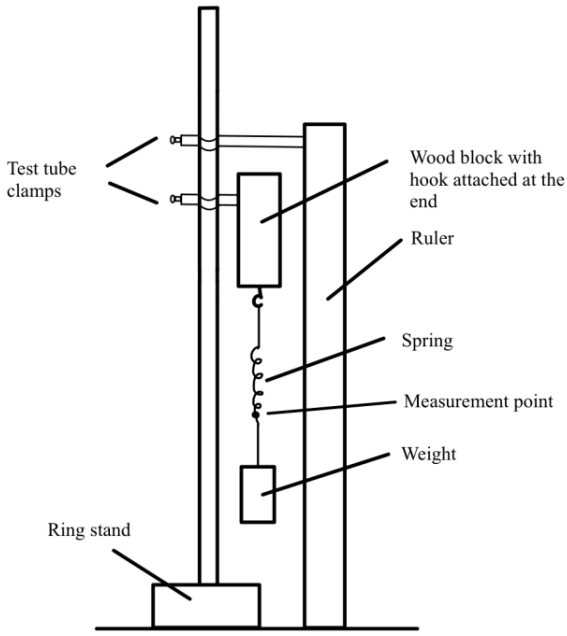

Figure 6: A suspended spring mass system that would allow the spring constant to be determined.

A wood block, with a hook at one end, is clamped facing down to a ring stand using a test tube clamp. A spring of constant k is suspended on the wood block, and 5 weights of different masses (10g, 20g, 30g, 40g, 50g) are hung on the spring respectively. A ruler is clamped to the ring stand using a test tube clamp, and is ensured to be parallel to the suspended spring to avoid inaccurate measurements. A point of measurement is marked towards the end of the spring with a marker as a reference point to make consistent measurements of its position. The spring's initial position was first measured by putting another ruler against the measurement point and lining it up with the reading

on the ruler. A weight was then suspended at the end of the spring and the spring's new position on the ruler measured. This process was repeated three times for each mass to minimize random errors.

The experiment follows Hooke's Law and the forces acting on the weight are as shown in Figure. 7,

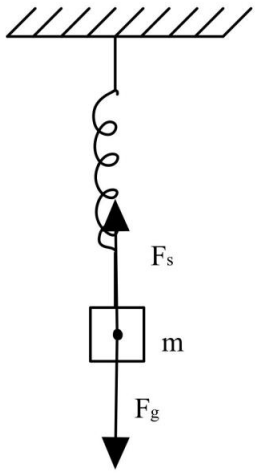

Figure 7: A mass m suspended by a spring with spring constant k, where the system is at rest as $F_s = F_g$

Figure. 7 shows that when the mass is suspended by the spring and is at rest, then $F_s = F_g$, or:

$$mg = -k(x - x_0)$$

Where x is the stretched position after hanging the mass and x_0 is the unstretched position. We let $\Delta x = x - x_0$ and rearranging the expression gives us:

$$\Delta x = -\frac{g}{k}m \tag{9}$$

The above equation suggests that there is a linear relationship between displacement and mass. We investigate this by plotting the displacement against mass (see Figure 8 from the measurements from the experiment described above,

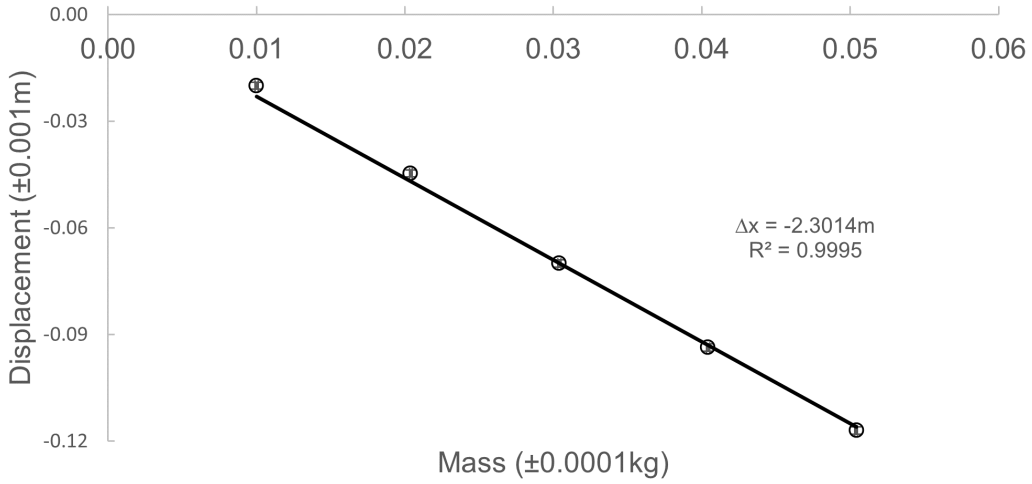

Figure 8: Results from the spring constant experiment where the displacement vs mass is plotted.

Figure 8 presents a strong linear relationship with a R^2 value of 0.9995. The included error bars are insignificant to have an effect on the slope of the graph. The slope from the linear regression: -2.3014, relates to the slope in Eq. 9: $-\frac{g}{k}$, where if we substitute the value 9.81 m/s^2 for g, the spring constant k comes out to be 4.2626 N/m.

Now we can derive the moment of inertia of our pendulum. The moment of inertia of a rigid body is the rotational mass that relates how difficult it is to change the angular velocity of a rotating body (Ling 524). It is denoted I and has a definition:

$$I = \sum_i m_i r_i^2 \tag{10}$$

Given that there are i number of mass elements that make up the shape, where m_i is the mass of a specific mass element and r_i is the distance from the axis of rotation to the mass element. We can apply this definition to our pendulum as shown in Figure 9,

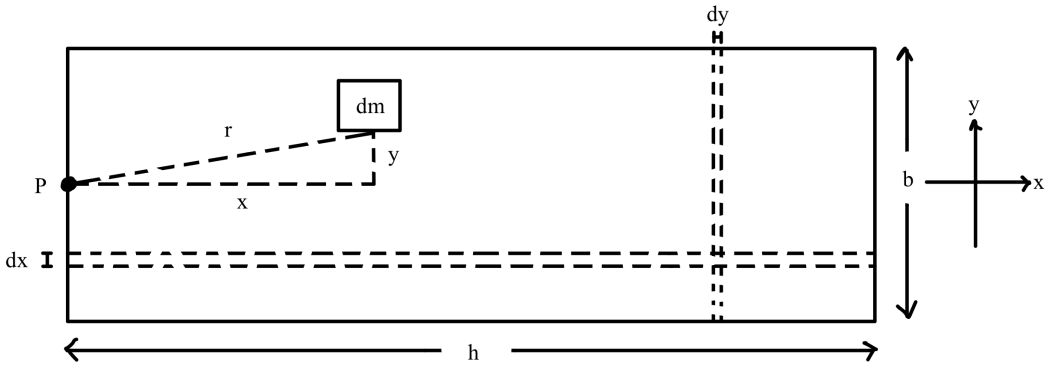

Figure 9: A two-dimensional view of the pendulum with an axis of rotation about the z-axis, and its length denoted h and height as b.

For the simplicity of our model, we have to make a few assumptions about our pendulum. The pendulum is assumed to have a rectangular shape with length h and width b; it is also assumed to have a uniform density; and the axis of rotation is assumed to be at the center of its width and edge of its length (point P in Figure 9).

The distance squared to each individual mass element can be written as, $r^2 = x^2 + y^2$. Assuming that there are k number of mass elements in the x axis, and n number of mass elements in the y axis, we can express the moment of inertia as the limit of an infinite Riemann Sum where the body is divided into an infinite number of mass elements in both planes:

$$I = \lim_{k,n\to\infty} \sum_{i=1}^{k} \sum_{j=1}^{n} (x_i^2 + y_j^2) m_{ij} \tag{11}$$

Where the mass m_{ij} relates to the spatial variables through the area mass density, ρ_A, defined as:

$$m_{ij} = \rho_A \frac{h}{k} \frac{b}{n} \tag{12}$$

The two fractions are related to $\Delta x = \dfrac{h}{k}$ and $\Delta y = \dfrac{b}{n}$ of the infinite Riemann Sum. Substituting Eq.12 into Eq.11:

$$\begin{aligned} I &= \lim_{k,n\to\infty} \sum_{i=1}^{k} \sum_{j=1}^{n} (x_i^2 + y_j^2) \rho_A \frac{h}{k} \frac{b}{n} \\ &= \rho_A \iint (x^2 + y^2) dx dy \end{aligned}$$

The upper and lower limits of these integrals can be inputted based on Figure.9:

$$I = \rho_A \int_{-b/2}^{b/2} \int_0^h (x^2 + y^2) dx dy$$

Where the area mass density, $\rho_A = \dfrac{m}{bh}$. Evaluating the double integrals gives us:

$$I = \frac{mh^2}{12}\left(4 + \frac{b^2}{h^2}\right) \tag{13}$$

All the parameters described in Eq. 13 were measured, where $m = 0.1383 \pm 0.0001$kg, $h = 0.4113 \pm 0.0005$m and $b = 0.0355 \pm 0.0005$m. We use these values to calculate the moment of inertia of our physical pendulum:

$$\begin{aligned} I &= \frac{(0.1383\,\text{kg})(0.4113\,\text{m})^2}{12}\left(4 + \frac{(0.0355\,\text{m})^2}{(0.4113\,\text{m})^2}\right) \\ &= 0.00781 \pm 0.00002\,\text{kgm}^2 \end{aligned}$$

5 Results and Analysis

With the theory and experimental processes discussed, we can compare our theory with the obtained experimental results, to see whether they agree. But first, we must look at how the videos were processed after the experiment. The videos were loaded into Tracker, which is a video analysis software that allows the motion of objects to be analyzed. A screenshot of the Tracker interface can be seen in Figure. 10,

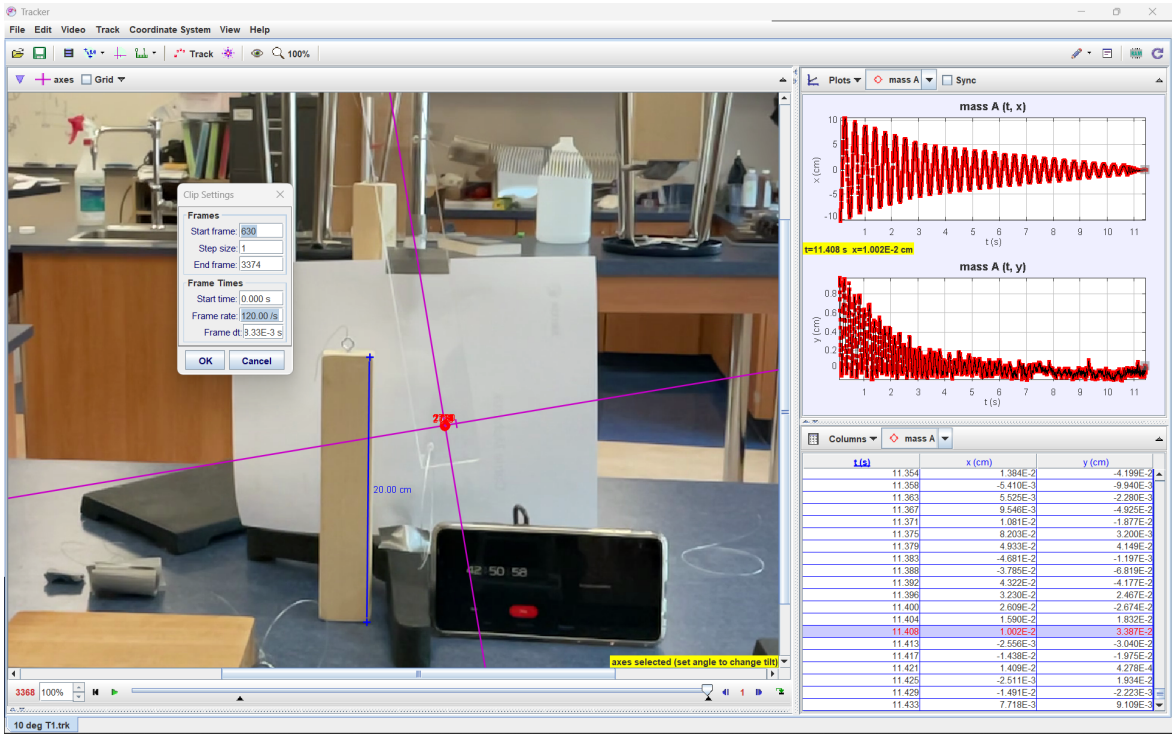

Figure 10: A screenshot of 10° trial 1 in Tracker, where the coordinate system (pink lines) was set at an angle of 9.5° from the vertical.

The frame rates of the video was set to 120fps, and the calibration stick specified to be 20.00cm. The purpose of the calibration stick is to adjust the video scale according to the objects' measurements. The coordinate system was moved, in adjustment of the equilibrium position, to the tracking point, and was set to be at an angle of 9.5° from the vertical.

By processing the videos on Tracker, we obtained the x and y positions of the tracking point; this allowed us to get the angular displacement by solving for θ. To verify our previously derived model, we fitted it to the experimental results by entering Eq. 6 into Excel and generate the angular displacement as a function of time with the measured parameters as shown in Figure 11,

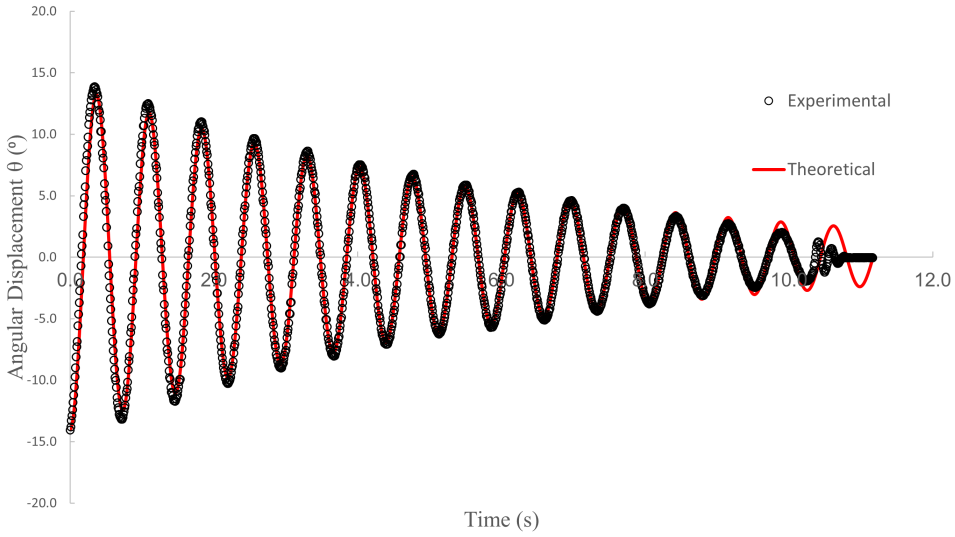

Figure 11: Eq. 6 fitted to the experimental data from 0° trial 1. The parameters used for Eq. 6 were: $m = 0.1383$kg, $r = 0.2408$m, $g = 9.81$m/s^2, $I = 0.00781$ kg/m^2 and $k = 4.2626$N/m

We determined the drag coefficient by minimizing the residual between the experimental and theoretical at each point in time. The returned value for drag coefficient produces the least deviation between the two data-sets. With the drag coefficient, we can determine the significance of drag force in the pendulum's period. From Figure 11, we can also determine our experimental period by averaging the time at a particular minimum t_n by the number of oscillations N, that is, $\frac{t_n}{N}$. However, the actual minimum point might not have been recorded with our setup, therefore, we computed a range uncertainty between its two neighboring points: t_{n-1} and t_{n+1}. This process was repeated for all trials and the averaged values are presented in Table 1,

Table 1: Measured and calculated values for φ, T and b

Angle $\varphi(^\circ)$	Measured $\varphi(\pm 0.01^\circ)$	Period T (s)	Drag Coefficient b (N/s)
0	0.08	0.733 ± 0.009	0.01057
10	9.78	0.738 ± 0.009	0.00750
20	19.75	0.749 ± 0.009	0.01153
30	30.20	0.758 ± 0.009	0.01600
40	39.73	0.799 ± 0.008	0.02364
50	49.70	0.834 ± 0.009	0.02540
60	59.83	0.898 ± 0.008	0.02856
70	69.40	0.960 ± 0.010	0.03025

The above table presents the measured φ from the inclinometer, and the averaged periods and drag coefficients. Plotting a graph of period T as a function of angle φ as shown in Figure 12,

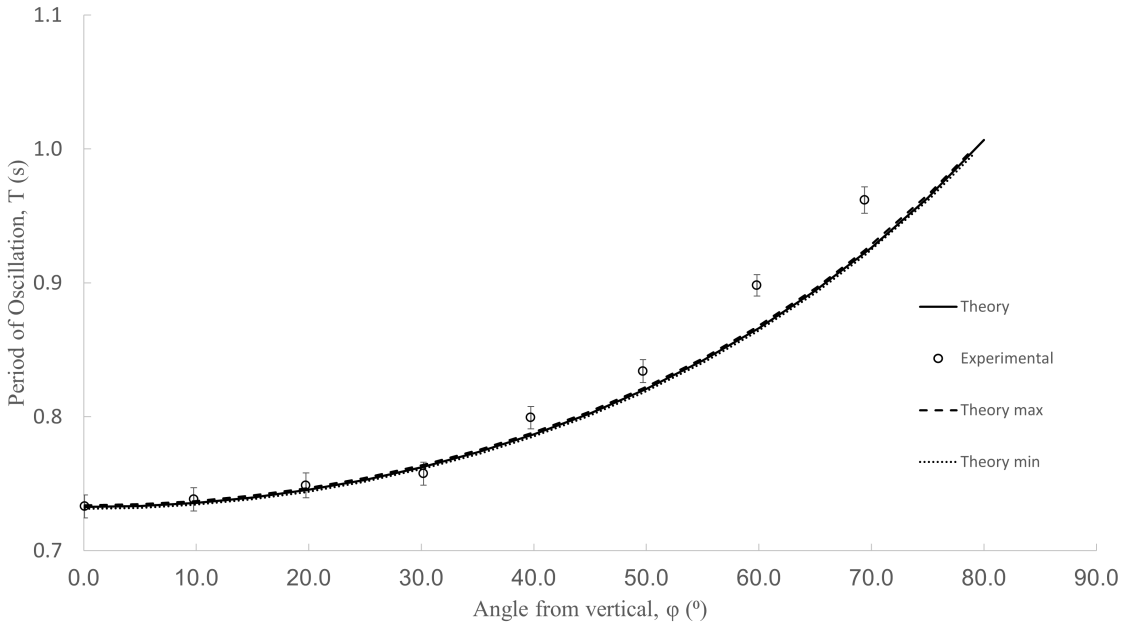

Figure 12: Relationship between the angle φ and the period of oscillation T

Figure 12 shows the relationship between the angle φ and the period of oscillation T. We computed the periods suggested by our model based on the assumption that the damping coefficient has insignificant effect on the period. It can be briefly shown by comparing the two terms in the damped frequency:

$$\omega_1 = \sqrt{\frac{kr^2 + mgr\cos\varphi}{I} - \left(\frac{br}{2I}\right)^2}$$

Substituting the values for these two terms will suggest that the first term is more than 400 times greater than the damping term. Therefore, we concluded that damping has an insignificant effect on the period, which allowed us to ignore the damping term and compute the period based on the system's natural frequency. We notice a trend in Figure 12, where the period increases with the inclination angle. This agrees our model (Eq. 8), because $\cos\varphi$ decreases as the angle increases, resulting in the denominator to decrease and period to increase. It is also noticed that at higher angles, starting from 40°, the experimental periods start to deviate from our model, which is also suggested by the increasing drag coefficients in Table 1. There are many possible explanations for this that are further discussed in Section 6, but we can explore whether errors play a role in our theoretical calculations. Since our model involves measured and calculated parameters that have uncertainties, we can propagate these errors to evaluate their significance. The 5 parameters are (k, r, I, m, φ), however, since we suggested that Fig 8 demonstrates a strong linear relationship with insignificant uncertainties, we can neglect

the error in the spring constant. Propagating the error in our model can be messy, so we separated this process into 3 steps: we can propagate the error for kr^2 first:

$$\begin{aligned}\Delta(kr^2) &= kr^2\left(2\frac{\Delta r}{r}\right)\\ &= (4.2626\text{N/m})(0.2408\text{m})^2\left(2\times\frac{0.0005\text{m}}{0.2408\text{m}}\right)\\ &= 0.001\text{Nm}\end{aligned}$$

We can propagate the error in $mgr\cos\varphi$, which gives us:

$$\Delta(mgr\cos\varphi) = (mgr\cos\varphi)\left(\frac{\Delta m}{m}+\frac{\Delta r}{r}+\frac{\Delta\cos\varphi}{\cos\varphi}\right)$$

The error in $\cos\varphi$ is associated with the maximum and minimum readings measured in the φ by the inclinometer. We can compute the range uncertainty provided by the output of the cosine function when taking in the maximum and minimum values. This gives us:

$$\begin{aligned}\Delta(mgr\cos\varphi) &= (0.1383\text{kg})(9.81\text{m/s}^2)(0.2408\text{m})(0.3518^\circ)\left(\frac{0.0001\text{kg}}{0.1383\text{kg}}+\frac{0.0005\text{m}}{0.2408\text{m}}+\frac{0.0002}{0.3518}\right)\\ &= 0.0004\text{Nm}\end{aligned}$$

Finally, we can propagate the error for the period:

$$\begin{aligned}\Delta T &= \frac{T}{2}\left(\frac{\Delta I}{I}+\frac{\Delta(kr^2)+\Delta(mgr\cos\varphi)}{kr^2+mgr\cos\varphi}\right)\\ &= \frac{0.922\text{s}}{2}\left(\frac{0.00002\text{kgm}^2}{0.00781\text{kgm}^2}+\frac{0.001\text{Nm}+0.0004\text{Nm}}{0.247\text{Nm}+0.1149\text{Nm}}\right)\\ &= 0.003\text{s}\end{aligned}$$

The propagated error in the period is used to plot a minimum and maximum period curves to compare whether the deviation at the higher angles are bounded by the error in our model. However, as seen in Figure 12, the error can be concluded to be insignificant as the maximum and minimum curves essentially overlap with the model.

6 Conclusion and Evaluation

In this investigation, we explored the relationship of period and inclination angle of our physical pendulum system. The process of modifying the traditional pendulum has led to several interesting insights. The addition of a spring leads to its inclusion in the period of our system, as it acts as an additional restoring force for our pendulum. Altering the pendulum's geometry also leads to the finding that our model suggests that the period increases in the form of $\frac{1}{\sqrt{\cos\varphi}}$ with inclination angle. However, our model starts to deviate at higher inclination angle. One possible explanation is the friction at the pivot point. It is possible that the pendulum is applying a greater normal force on the shaft at higher inclination angles, as there is less support towards the bottom part of the pendulum, potentially bending the pendulum. It is exceptionally possible as our pendulum is relatively long in length, the support towards the end can be significantly less than the part near the pivot. We can assume this is a plausible reason as the pendulum is also observed to be bent more at increasing inclination angles towards the bottom part. This factor leads to greater friction at the pivot point and greater drag force, therefore, the drag coefficient increases. To investigate the effect of length of a rotating rigid body, we can experiment with pendulums that are of longer lengths. We can thus be able to see a more noticeable bend in the rod, and investigate whether rigid bodies of longer lengths increase the friction at the pivot point, therefore, increasing the damping coefficient at higher inclination angles. Since our model did not consist of the friction at the pivot point, we can propose the explicit inclusion of frictional force in our model. We can account for the friction generated by the specific material of the shaft or the roughness of the two contacting surfaces. We can also experiment with the addition of lubricants (E.g. WD-40) to see whether it reduces the drag coefficient.

In this investigation, we have made a few assumptions in order to simplify our model; however, these assumptions can also lead to potential inaccuracies. For instance, we assumed that the drag force experienced at the center of mass is proportional to the drag coefficient. Although this is a conventional assumption, we can propose that due to our pendulum being a rigid body, it experiences a drag forces of different magnitudes along its body. This is because the mass elements along the body are at different velocities; the mass elements closer to the pivot have lower velocities, therefore, they consequently experience less drag force. We can test the effect of different drag forces along the pendulum's body by replicating our pendulum, rotating in air, in a simulation. This allows us to divide the pendulum into different pieces that experience different velocities; finally, letting us compute to see whether there is a significant deviation in the drag force in comparison to our model.

We also made an assumption that our pendulum is perfectly rectangular and have a uniform

density along its body; however, it is only for the simplicity of our model. In our experiment, the pendulum is a combination of many different shapes and has greater mass towards the pivot point. These factors could have affected the drag experienced by the pendulum, friction at the pivot point, and the calculation of its moment of inertia. We can investigate this effect by creating a rigid body that has the same dimensions used in the calculations of this paper, and determine whether our assumptions impacted the results.

Works Cited

Feliciano, José. “The Variable Gravity Pendulum.” *American Association of Physics Teachers*, American Association of Physics TeachersAAPT, 1 Jan. 1998, https://aapt.scitation.org/doi/10.1119/1.879963.

Lehman. https://www.lehman.edu/faculty/anchordoqui/chapter24.pdf.

Libretexts. “6.7: Drag Force and Terminal Speed.” *Physics LibreTexts*, Libretexts, 12 Sept. 2022, https://phys.libretexts.org/Bookshelves/University_Physics/Book%3A_University_Physics_(OpenStax)/Book%3A_University_Physics_I_-_Mechanics_Sound_Oscillations_and_Waves_(OpenStax)/06%3A_Applications_of_Newton's_Laws/6.07%3A_Drag_Force_and_Terminal_Speed.

Ling, Samuel J., et al. *University Physics: Volume 1*, OpenStax, Rice University, Houston, TX, 2017, p. 524.

Ling, Samuel, et al. *University Physics: Volume 1*, OpenStax, Rice University, Houston, TX, 2017, pp. 508–509.

Tsokos, K. A. *Physics for the IB Diploma*, Cambridge University Press, Cambridge, 2016, pp. 49–50.